論文 한국정밀공학회지 제 12 권 제 2 호 1995. 2
Journal of the Korean Society of Precision Engineering Vol. 12. No 2. February. 1995.

룰 방식에 의한 조립경로 생성 및 이동용 로봇에의 적용

이 병 룡*

Rule-Based Path Finding Algorithm for Part Assembly and Its Extension to Mobile Robot Path Planning

Byung-Ryong Lee*

ABSTRACT

조립작업에 있어서의 경로계획(path planning)에 대하여 지금까지 많은 연구가 진행되어 왔으며, 그것의 주종을 이루는 것들은 cell decomposition 방식과 potential field 방식이다. 그러나, 이러한 방식들은 free space를 세분하거나 potential field를 계산하는데 많은 시간을 필요로 하며, 조립부품 이동영역이 configuration space로 먼저 치환이 되어야 하는 문제점들이 발생하게 된다. 그러므로, 만약에 조립부품에 대한 이동환경이 복잡하지 않고 알려져 있으면 위의 방식들은 비용적인 면에서 많은 낭비를 가져온다. 본 논문에서는 간단하면서도 알려진 작업환경에서 효과적인 조립부품의 경로계획 알고리즘을 개발하였다. 먼저, channel, junction 및 간격 유지계수(clearance gap)의 개념을 도입하고, 이 개념들을 이용하여 룰 방식의 알고리즘을 개발하였다. 그리고, 이 알고리즘을 이동용 로봇의 경로계획에도 적용될 수 있음을 보였다.

1. Introduction

Two main methods of path planning are the cell decomposition method[1][2][3][4] and the potential field method.[5][6][7] The cell decomposition method decomposes free space, where no collision occurs, into simple regions called cells. Then, a non-direct graph representing the adjacency relation between the cells is constructed and searched. The potential field method uses artificial potential fields applied to the obstacles and goal position and uses the resulting field to influence the path of the object which is subject to this potential. However, these approaches usually require huge computational time to decompose and refine the free-space or to develop the artificial potential field, and in both approaches the moving space of the assembly part should be substituted into the configuration space.[8] Therefore, if the moving environment for assembly part is known and simple, the above approaches are too expensive to use. In this paper, first, an assembly path-finding algorithm for male and female parts is proposed using only vertices of the male and female

* 한국기계연구원 지동화연구부

parts when their initial and goal positions are known. In the simple assembly case the relative relationship of the two parts can be easily represented by considering vertices. And the free-space inside the female part is approximated using channels and junctions which are similar to pipes and elbows of water pipe lines. An algorithm is developed to find a simple and efficient disassembly path of the male part in the approximated free-space of the female part. In this algorithm priority between the safe path and the short path can be easily selected using pre-defined clearance gap. Once the disassembly path is found, the corresponding assembly path can be found by reversing the sequence of the disassembly path. [9][10]

Next, the disassembly path planning developed above will be extended to fit mobile robot path planning. Here, the male part(or mobile robot)can move in the negative Z-direction and it has both translational and rotational motion. First, path-finding algorithm for mobile robot will be developed by using the geometrical relationship between junctions and channels. Then, two numerical examples to find the paths of the mobile robot in the two different corridor problems will be graphically demonstrated.

2. Modeling of Free-Space for Part Assembly

The male part and female part will be considered throughout this paper. Here, the male part is defined as a part which is inserted into the other part during the parts assembly task, and the female part is defined as a part into which the other part is inserted during the part assembly task. In parts assembly, because the male part should be assembled into the female part without any collision, the inside of the female part can be considered as free-space for the male part. In this section, the basic concept of approximate cell decomposition method is used to represent free-space. Unlike the classical method of approximate cell decomposition which uses quadtree or octree decomposition to generate a more precise approximation of a free space with much smaller cells, this technique uses rectangloid cells[11][12] to simplify a free-space. Hence, this technique is much more efficient and needs less computation. In this section channel and junction are introduced to represent simplified free-space inside female part. Channel and junction are kinds of rectangloids which can be represented by half-spaces. In the 2-dimensional case, all rectangloids can be represented by using four half-spaces. Here, half-spaces are defined as follows:

$$H_s(\bar{s})^+ = \{P : P_s \geq \bar{s}\} \qquad (2.1)$$
$$H_s(\bar{s})^- = \{P : P_s \leq \bar{s}\}$$

, where the subscript s denotes the principal coordinate, i.e., x or z in the 2-dimensional case, and $\bar{s}$ denotes an arbitrary constant value. P_s denotes s-coordinate value of a point P, and { } denotes a mathematical set. Then a channel, denoted as C, can be described as the intersection of four half-spaces:

$$c = H_x(x_1)^+ \cap H_x(x_2)^- \cap H_z(z_1)^+ \cap H_z(z_2)^- \quad (2.2)$$

, where x_1, x_2, z_1 and z_2 are arbitrary constant value such that $x_1 < x_2$ and $z_1 < z_2$. Then, the approximated free-space inside the female part can be described as the unions of channels:

$$S_{fs} = \bigcup_{i=1}^{n} C_i \qquad (2.3)$$

, where S_{fs} denotes the approximated free-space, and n denotes the total number of channles that consist of the simplified free-space. In Equation (2.3), two consecutive channels should be "L" shaped orthogonal, and

have a non-empty intersection that is $C_i \cap C_{i+1} \neq \emptyset$. From this requirements, *junction* (J_i) is defined as

$$J_i = C_i \cap C_{i+1}, \quad i = 1,2,...,n-1 \qquad (2.4)$$

In this paper, it is considered that the male part has only translational motion in the free-space. Hence, for a successful disassembly task in the free-space, every junction must satisfy the following conditions:

$$\max\_width(J_i) > \max\_width(M) \qquad (2.5)$$
$$\max\_height(J_i) > \max\_height(M)$$

, where M denotes the male part, and max_width(.) and max_height(.) denote the maximum width and maximum height of the i^{th} junction or the male part, respectively. Fig. 1 shows an example of free-space modeling using channels and junctions. Here, channels and junctions can be described as

$$C_1 = H_x(x_1)^+ \cap H_x(x_2)^- \cap H_z(z_2)^+ \cap H_z(z_4)^- \quad (2.6)$$
$$C_2 = H_x(x_1)^+ \cap H_x(x_4)^- \cap H_z(z_2)^+ \cap H_z(z_3)^-$$
$$C_3 = H_x(x_3)^+ \cap H_x(x_4)^- \cap H_z(z_1)^+ \cap H_z(z_3)^-$$
$$J_1 = C_1 \cap C_2, \quad J_2 = C_2 \cap C_3$$

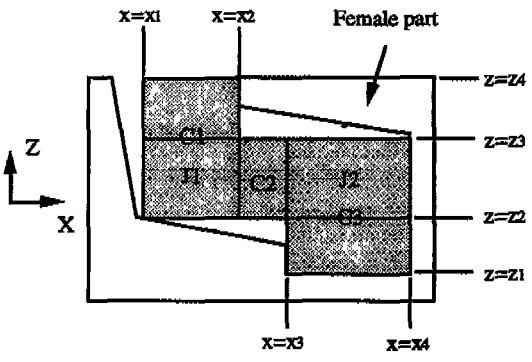

Fig. 1 An example of simplified free-space representation

3. Disassembly Path Planning

In the previous section, the free-space inside a female part was modeled by using channels and junctions. This modeling scheme is very simple and easy to develop a path-finding algorithm. In this section, using the free-space model a simple and efficient path-finding algorithm is developed. A numerical example is given to test the feasibility of the path-finding algorithm.

In order to arrive at an algorithm, some definitions associated with the disassembly procedure are defined. Based on these definitions a path-finding algorithm is developed from the geometrical relationship between the free-space and a male part.

Definition 3.1

If a male part is located at the end state of assembly task or at the initial state of the disassembly task, then the male part is said to be in *assembled state*.

Definition 3.2

If a male part begins to satisfy the condition such that $\min\{M_z\} > \max\{(S_{fs})_z\}$, the male part is said to be in *disassembled state*, where $\{M_z\}$ and $\{(S_{fs})_z\}$ denote z-coordinate value sets for the vertices of the male part and the free-space, respectively.

In definition 3.2, x-z coordinate is chosen so that the line passing through the center positions of the first channel and the first junction in the assembly sequence could be parallel to the z-direction, and that the center position of the first channel is more positive side in z-direction than that of the first junction. A general sequence of disassembly path is described as follows:

ASSEMBLED STATE ⇒ N^{th} JUNCTION ⇒ ...
⇒ 1^{st} JUNCTION ⇒ DISASSEMBLED STATE

, where the N^{th} junction and the 1^{st} junction are the junctions closest to the assembled state and the disassembled state, respectively, and $\Rightarrow$ denotes the flow of disassembly. In the disassembly path, the change of the directional movement of the male part happens only in each junction, and each junction also contains the geometrical information between the two consecutive channels. Hence, the path-finding algorithm can be developed by considering the positional relationship between the junctions and the male part.

Adjustable clearance gap

According to condition (2.5), the area of any junction has to be greater than that of the male part for a successful disassembly in the approximated free-space. Hence, there exist many target positions that the male part can assume within the next junction. In some case, a shortest path is desired to reduce the length of the total traveled path. In other cases, a collision-free path is desired if a collision is to be avoided at all cost. Hence, *Adjustable clearance gap* between the male part and the corresponding junction is defined as the following conditions:

$$0 < (gap\_x)_{J_i} < (WIDTH(J_i) - WIDTH(M_i))/2.0 \quad (3.1)$$
$$0 < (gap\_z)_{J_i} < (HEIGHT(J_i) - HEIGHT(M_i))/2.0$$

, where $(gap\_x)_{J_i}$ and $(gap\_z)_{J_i}$ denote clearance gaps in the x and z directions, respectively, in the i^{th} junction. In condition (3.1), if the shorter travel path is desired, the clearance gaps should be close to zero. On the other hand, if the safer travel path is desired, the clearance gaps should be close to the maximum value of the allowable clearance gap.

Rules to find the target position in the next junction

There exist many directional vectors for the male part as it moves from its current junction to the next junction. The rules to find the target position of the male part in the next junction are shown in Table 1. In Table 1, $\{J(I)_x\}$ denotes the set of x-coordinate values of the junction for the male part to enter, and $\{M_x\}$ denotes the set of x-coordinate values of all vertices of the male part in the current position. $\{J(I-1)_x\}$ denotes the set of x-coordinate values of junction J(I-1). For simplicity, it is assumed that the male part does not have a directional vector in the negative z-direction so that the two consecutive junctions satisfy the following condition:

$$\max\{J(I-1)_z\} \geq \max\{J(I)_z\} \quad (3.2)$$

Hence, the moving direction and target position of the male part in the next junction can be calculated from the relationship of male part M, junction J(I), and junction J(I-1). For example, as shown in Fig. 2, when the male part is at M position, its new position M_i has left-margined gap_x and down-margined gap_z from Table 1

Next, the movable distance in the x and z directions from the current junction to the next junction can be easily calculated by using

Table 1 Rules to find the target position of the male part in the next junction

	relationship between male part and junctions	target position in next junction
Rule 1	If $\min\{J(I)_x\} < \text{all}\{M_x\} < \max\{J(I)_x\}$ $\max\{J(I-1)_x\} < \max\{J(I)_x\}$	Then, left-margined gap_x down-margined gap_z
Rule 2	If $\min\{J(I)_x\} < \text{all}\{M_x\} < \max\{J(I)_x\}$ $\max\{J(I-1)_x\} > \max\{J(I)_x\}$	Then, right-margined gap_x down-margined gap_z
Rule 3	If $\min\{J(I)_z\} < \text{all}\{M_z\} < \max\{J(I)_z\}$ $\max\{J(I)_x\} < \max\{M_x\}$	Then, right-margined gap_x up-margined gap_z
Rule 4	If $\min\{J(I)_z\} < \text{all}\{M_z\} < \max\{J(I)_z\}$ $\max\{J(I)_x\} > \max\{M_x\}$	Then, left-margined gap_x up-margined gap_z

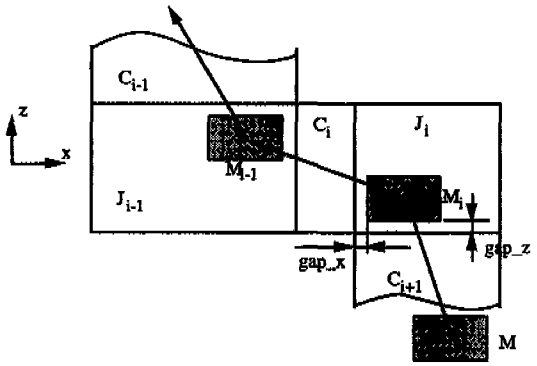

Fig. 2 An example to find the target position in the next junction

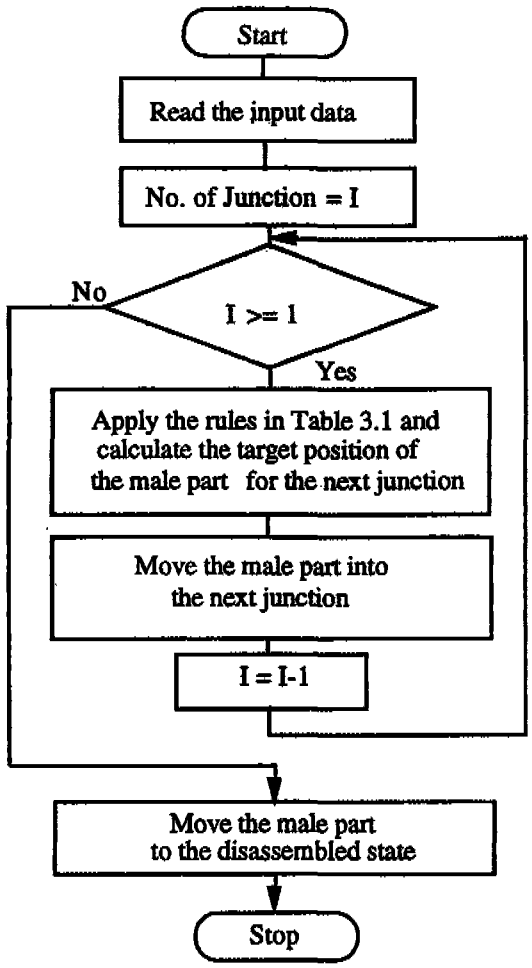

Fig. 3 The flowchart of the disassembly path-finding algorithm

the rules in Table 1. For example, considering the Rule 1 in Table 1, the movable distances in the x and z directions (mdx, mdz) can be derived from the following equations:

$$mdx = \min\{J(I)_x\} + gap\_x - \min\{M_x\} \quad (3.3)$$
$$mdz = \min\{J(I)_z\} + gap\_z - \min\{M_z\}$$

The flowchart of the disassembly path-finding algorithm is illustrated in Fig. 3. This algorithm continues to find the target position of the male part for the subsequent junctions in the disassembly sequence until the male part reaches junction 1 which is the junction closest to the disassembled state. From there, the disassembled state can be reached in one directional motion.

4. Numerical Examples

Let's consider a male part M and a female part F at the assembled(initial) state as shown in Fig. 4. In this figure, the vertices data for the male and the female part, and the boundary data of the free-space are given in X-Z coordinate. Here, all the data are expressed based on the reference point, f_1=(0, 0). All the vertices data of the female and the male parts are given as follows:

$f_1 = (0,0)$, $f_2 = (0,7)$, $f_3 = (1,7)$, $f_4 = (1,2)$
$f_5 = (4,2)$, $f_6 = (4,1)$, $f_7 = (7,1)$, $f_8 = (7,6)$
$f_9 = (5,6)$, $f_{10} = (5,7)$, $f_{11} = (8,7)$, $f_{12} = (8,0)$
$m_1 = (4.5,1.01)$, $m_2 = (4.5,4)$, $m_3 = (6.99,4)$
$m_4 = (6.99,1.01)$

and the boundary line data for the channels and the junctions are given as

$h_0 = (x,7)$, $h_1 = (1,z)$, $h_2 = (5,z)$, $h_3 = (x,2)$
$h_4 = (x,6)$, $h_5 = (4,z)$, $h_6 = (7,z)$, $h_7 = (x,1)$

In Fig. 4, junction 1 is the space which consists of h_1, h_2, h_3, and h_4. And, junction 2 is the space which consists of h_3, h_4, h_5, and h_6.

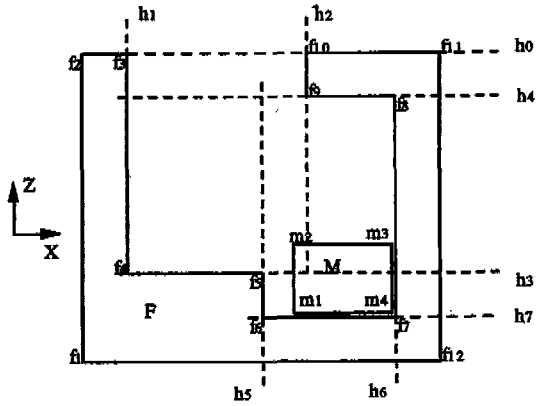

Fig. 4 Schematic diagram for male and female parts in initial state

If the vertex data of the reference point f_1 is given with respect to the base frame (X, Z), all other vertices data of parts M and F and the boundary data of the half-space can be expressed on the base frame. In this example, the reference point at the initial (i.e., disassembled) state is chosen as f_{1i}=(12, -6), and the position of f_1 at the final(i.e., disassembled) state is given as f_{1f}=(14, 1). Here, data f_{1i} and f_{1f} are expressed with respect to the base frame (X, Z). In this example, the disassembly paths of the male part are simulated for the 3 cases of clearance gaps with 0.01, 0.2, and the safest gap. And their graphical results are shown in Fig. 5

5. Extension to Mobile Robot Path Planning

In previous section disassembly path planning was introduced, where it was assumed that the motion of the male part is translational and the male part does not move in the negative z direction. In this chapter it is considered that the male part has both translational and rotational motion and it can move in the negative z direction. Therefore, this kind of male part motion can be applied to

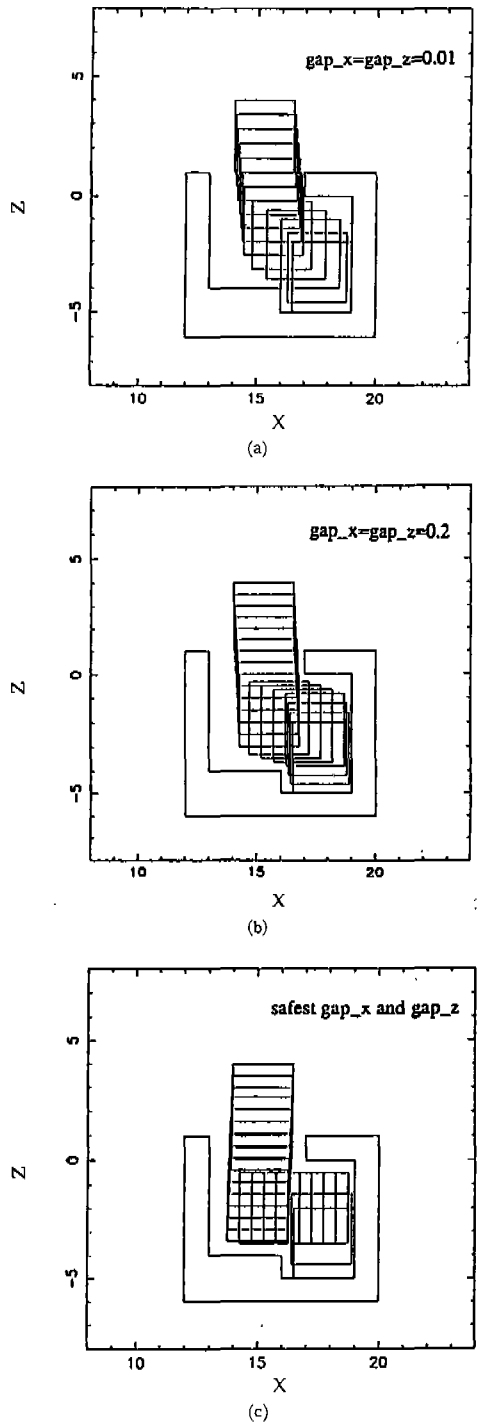

Fig. 5 Disassembly path for different clearance gaps
a) gap_x=gap_z=0.01 b) gap_x=gap_z=0.2
c) safest gap_x and gap_z

the path planning of a mobile robot or an AGV which moves in a corridor.

5.1 Path-Finding Algorithm for Mobile Robot

In the previous section the free-space inside a female part was modeled by using channels and junctions, from which a simple and efficient path-finding algorithm was developed. In this section the basic idea will be extended to the path planning for a mobile robot by considering the translational/rotational motion. At first, the guiding curve of the mobile robot in a junction is defined as a quarter circle whose radius is

$$\rho = \frac{w}{2} + gap\_r, \tag{5.1}$$

where ρ is the radius of the guiding curve in the entering junction, w is the width of a mobile robot, and gap_r is denoted as a radial clearance gap. Through this chapter, a mobile robot will be considered as a rectangular shape. Therefore, the width w is constant during the motion. In previous section, the clearance gap in the x and z direcions were defined as in condition (3.1). However, in this section the radial clearance gap will be defined as the length of the radius with respect to a corner point in the junction. When the center point of the mobile robot arrives at a position on the guiding circle, the center point moves along the guiding curve, keeping the center line of the mobile robot tangent to the guiding curve, and the center point of the mobile robot leaves the curve at a position on the guiding curve.

These two positions on the guiding curve will be defined hereafter as an *arriving point* and a *leaving point* on the guiding curve. The points can be calculated from the relationship between the entering junction and the next junction, and the current position of the mobile robot. The entering junction is the junction which the mobile robot is about to enter. Before developing the general rules for finding the arriving and leaving points in the entering junction, a specific configuration as shown in Fig. 6 will be analyzed, from which all possible rules will be developed.

In Fig. 6, if m_0 is the center point of the rectangular mobile robot at its current state, the arriving angle, Θ_a, is calculated as

$$\Theta_a = \cos^{-1}\frac{\rho}{1_{mp}} - \cos^{-1}\frac{(p_n)_x - (m_0)_x}{1_{mp}} \tag{5.2}$$

where ρ is the radius of the guiding curve, p_n is the corner point of the entering junction n, and 1_{mp} is the length between m_0 and p_n. Similarly, the leaving angle Θ_1, is defined as

$$\Theta_1 = \cos^{-1}\frac{2\rho}{1_{pp}} - \cos^{-1}\frac{(p_{n-1})_y - (p_n)_y}{1_{pp}} \tag{5.3}$$

where 1_{pp} is the length between two corner points p_n and p_{n-1}. Hence, the arriving point, m_a, on the guiding curve can be calculated as

$$\begin{aligned}(m_a)_x &= (p_n)_x - \rho.\cos\Theta_a \\ (m_a)_y &= (p_n)_y + \rho.\sin\Theta_a\end{aligned} \tag{5.4}$$

The mobile robot moves from its current position to the arriving point such that the

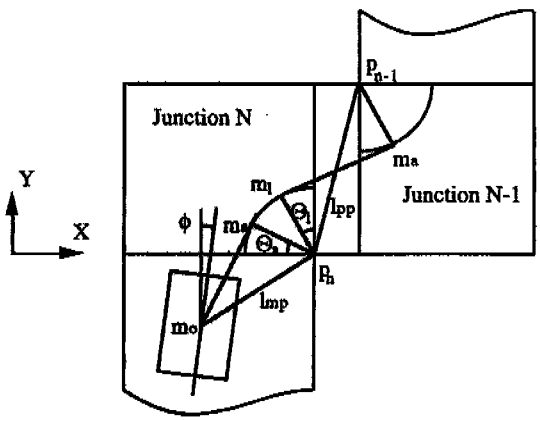

Fig. 6 The mobile robot motion in a specific configuration

center point m_0 follows the line connecting m_0 and m_a, and during the motion the rotating angle of the mobile robot is $\Theta_a - \phi$ degrees, where ϕ denotes the configuration angle of the mobile robot at its current position. Once, the center point of the mobile robot reaches the arriving point m_a, it moves along the arc connecting m_a and m_1, and during the motion the rotating angle of the mobile robot is $90 - \Theta_a - \Theta_1$ degrees with the center line of the mobile robot keeping tangent to the arc.

Using the procedure from Equation (5.2) to Equation (5.4), the arriving points on the guiding curves for all possible configurations of junctions can be defined. Table 2 shows the rules for finding the arriving point for all possible configurations.

In Table 2, $(J_n)_x$ denotes the average x-coordinate value of junction N(i.e., entering junction), and $(M)_x$ denotes the average x-coordinate value of the mobile robot at current position. The notations of the arriving points are described as follows:

$$(m_a)_x^+ = (p_n)_x + \rho.\cos\Theta_a \qquad (5.5)$$
$$(m_a)_x^- = (p_n)_x - \rho.\cos\Theta_a$$
$$(m_a)_y^+ = (p_n)_y + \rho.\sin\Theta_a$$
$$(m_a)_y^- = (p_n)_y - \rho.\cos\Theta_a$$

where from rule 1 to rule 4 the arriving angle, Θ_a, is defined as

Table 2 Rules to find the arriving point on the guiding curve

Rules	Condition	Arriving Point
Rules 1	IF $(J_n)_x < (J_{n-1})_x$ & IF $(J_n)_y > (M)_y$,	THEN $(m_a)_x^-$ & $(m_a)_y^-$
Rules 2	IF $(J_n)_x < (J_{n-1})_x$ & IF $(J_n)_y < (M)_y$,	THEN $(m_a)_x^-$ & $(m_a)_y^+$
Rules 3	IF $(J_n)_x > (J_{n-1})_x$ & IF $(J_n)_y > (M)_y$,	THEN $(m_a)_x^+$ & $(m_a)_y^-$
Rules 4	IF $(J_n)_x > (J_{n-1})_x$ & IF $(J_n)_y < (M)_y$,	THEN $(m_a)_x^+$ & $(m_a)_y^+$
Rules 5	IF $(J_n)_y < (J_{n-1})_y$ & IF $(J_n)_x > (M)_x$,	THEN $(m_a)_x^+$ & $(m_a)_y^-$
Rules 6	IF $(J_n)_y < (J_{n-1})_y$ & IF $(J_n)_x < (M)_x$,	THEN $(m_a)_x^-$ & $(m_a)_y^-$
Rules 7	IF $(J_n)_y > (J_{n-1})_y$ & IF $(J_n)_x > (M)_x$,	THEN $(m_a)_x^+$ & $(m_a)_y^+$
Rules 8	IF $(J_n)_y > (J_{n-1})_y$ & IF $(J_n)_x < (M)_x$,	THEN $(m_a)_x^-$ & $(m_a)_y^+$

$$\Theta_a = \cos^{-1}\frac{\rho}{1_{mp}} - \cos^{-1}\frac{|(p_n)_x - (m_0)_x|}{1_{mp}} \qquad (5.6)$$

and from rule 5 to rule 8 the arriving angle, Θ_a, is defined as

$$\Theta_a = \cos^{-1}\frac{\rho}{1_{mp}} - \cos^{-1}\frac{|(p_n)_y - (m_0)_y|}{1_{mp}} \qquad (5.7)$$

Using the eight rules as illustrated in Table 2, the path-finding algorithm for mobile robot in corridor problems can be developed. The simple flowchart of the path planning algorithm is shown in Fig. 7

5.2 Numerical examples

In this section two numerical examples for finding the paths of the mobile robot in two different corridor problems will be demon-

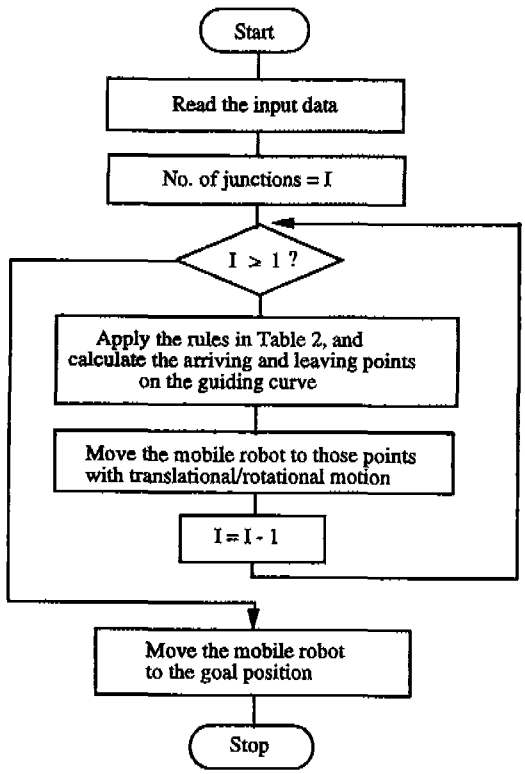

Fig. 7 The flowchart of the path-finding algorithm for the mobile robot

strated. Here, the input information is the vertices data of each junction and the initial and goal positions of the mobile robot. The mobile robot is chosen as width=1.0 and height=1.5. In each example, 3 cases of clearance gaps with 0.2, 0.6 and 1.0 are used to show how the path of the mobile robot depends on the value of the clearance gap. The rseults of the examples are shown in Fig. 8. In these examples it is easily observed that the mobile robot turns every corner point with the given clearance gap, and the path patterns are also changed by the clearance gaps. If the clearance gap becomes smaller, the travel path of the mobile robot becomes shorter. But, in the practical point of view, because of some uncertainty problem, there may exist a collision between the mobile robot and the corner point of the entering junction. On the other hand, if the clearance gap becomes larger, the travel path of the mobile robot becomes longer, but the possibility of colliding with the corner point will be less. One problem is that the mobile robot will also become closer to the opposite wall of the junction as the clearance gap becomes larger. Therefore, in order to find the clearance gap which gives the safest path, trial and error is necessary. The major advantage of this algorithm is that diverse paths can be found by only changing the clearance gap. However, this algorithm is limited, in that it can be applied only to specific corridor problems.

6. Conclusion

In this paper, an assembly path planning was developed. Here, the inside free-space of the female part was simplified into a series of rectangular spaces using junctions and channels, from which a simple and efficient assembly path planning algorithm was devel-

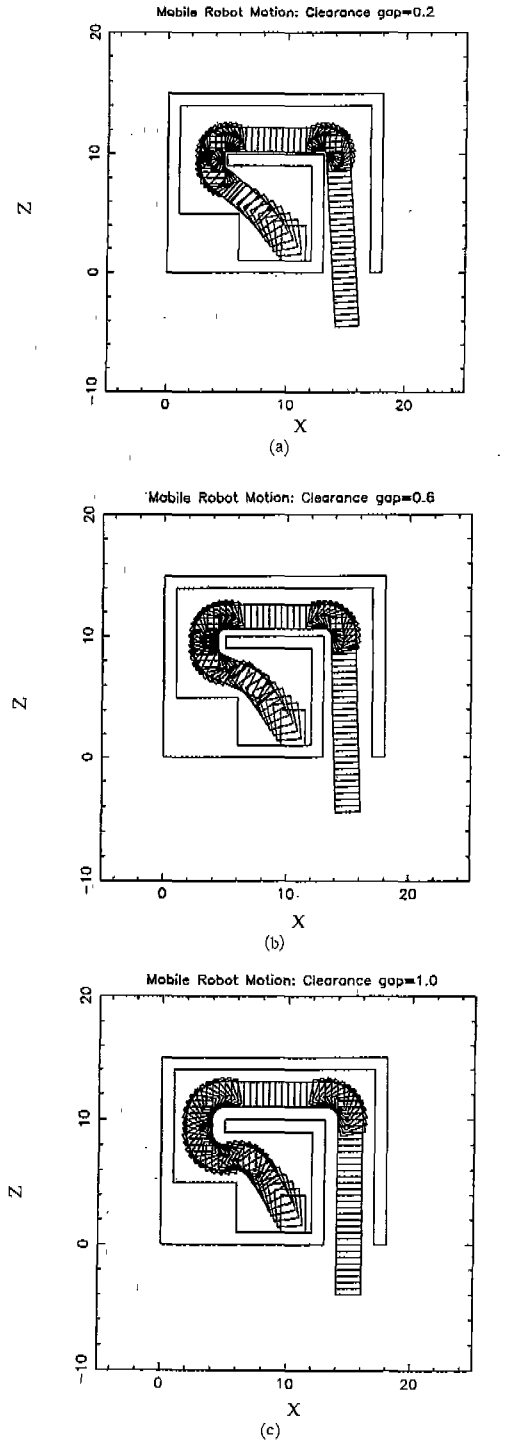

Fig. 8. Mobile Robot Paths with different clearance gaps clearance gaps: a) 0.2 b) 0.6 c) 1.0

oped. As this algorithm exploits some decision rules based on the geometrical relation of the junctions and the male part, the computation effort can be greatly reduced, compared to the configuration space or the classical cell decomposition method. The other advantages of this algorithm are that it can be easily extended to the 3-dimensional case by just adding some additional rules and it can get any desired disassembly path by just changing the clearance gap in the junctions. The disassembly path planning can be extended to fit mobile robot path planning in the rectangular corridor problem. This algorithm deals with both translational and rotational motions. However, this algorithm has a limitation that, in some cases, it is impossible to model the inside free-space of the female part into simplified rectangular space where the male part can move.

References

1. J.T. Schwartz and M. sharir, "On the Piano Moves' Problem: I, The Case of a Two-Dimensional Rigid Polygonal Body Moving Amidst Polygonal Barriers", Communication on Pure and Applied Mathematics, Vol. 34, 1983, pp. 345-398.
2. F. Avnaim, J.D. Boissonnat and B. Faverjon, "A Pracitical Exact Motion Planning Algorithm for Polygonal Objects Amidst Polygonal Obstacles, Technical Report No. 890, INRIA, Sophia-Antipolis, France, 1988."
3. J. Faverjon, P. Tournassoud, "A Practical Approach to Motion Planning for Manipulators with many Degrees of freedom", 5th International Symposium of Robotics Research, 1989, pp. 65-73.
4. C. Laugier, F. Germain, "An Adaptive Collision-Free Trajectory Planner", Proceedings of International Conference on Advanced Robot", 1985.
5. O. Khatib, "Real-time Obstacle Avoidance for Manipulators and Mobile Robots", Int. J. of Robotics Research, 5(1), 1986, pp. 90-98.
6. Y. K. Hwang and N. Ahuja, "A Potential field Approach to Path Planning", IEEE Transaction on Robotics and Automation, Vol. 8, No. 1, 1992, pp. 23-32.
7. C. W. Warren, "Multiple Robot Path Coordination Using Artificial Potential Fields", IEEE International Conference of Robotics and Automation, 1990, pp. 500-505.
8. R. A. Brooks and T. Lozano-perez, "A Subdivision Algorithm in Configuration Space for Findpath with Rotation", Int. Joint Conf. on Artificial Intelligence, 1983, pp. 799-806
9. Y. F. Huang and C. S. G. Lee, "A Framework of Knowledge-Based Assembly Planning", IEEE Int. Conf. on Robotics and Automation, 1991, pp. 599-604.
10. Y. Liu and R. J. Popplestone, "Symmetry Groups in analysis of Assembly kinematics", IEEE International Conference on Robotics and Automation, 1991, pp. 572-577.
11. S. J. Jun, K. G. Shin, "Shortest Path Planning with Dominance Relation", IEEE International Conference on Robotics and Automation, 1990, pp. 138-143.
12. D. Zhu, J. Latombe, "Pipe Routing = Path Planning", IEEE International Conference on Robotics and Automation, 1991, pp. 1940-1947.